Published in final edited form as:
J Comp Physiol A Neuroethol Sens Neural Behav Physiol. 2013 November ; 199(11): . doi:10.1007/s00359-013-0849-z.

Synchronous firing of antennal-lobe projection neurons encodes the behaviorally effective ratio of sex-pheromone components in male *Manduca sexta*

Joshua P. Martin[1], **Hong Lei**[2], **Jeffrey A. Riffell**[3], and **John G. Hildebrand**[2]

[1]Department of Biology, Case Western Reserve University, 10900 Euclid Avenue, Cleveland, Ohio 44106, USA

[2]Department of Neuroscience, University of Arizona, PO Box 210077, Tucson, Arizona 85721, USA

[3]Department of Biology, University of Washington, PO Box 351800, Seattle, Washington 98195, USA

Abstract

Olfactory stimuli that are essential to an animal's survival and reproduction are often complex mixtures of volatile organic compounds in characteristic proportions. Here, we investigated how these proportions are encoded in the primary olfactory processing center, the antennal lobe (AL), of male *Manduca sexta* moths. Two key components of the female's sex pheromone, present in an approximately 2:1 ratio, are processed in each of two neighboring glomeruli in the macroglomerular complex (MGC) of males of this species. In wind-tunnel flight experiments, males exhibited behavioral selectivity for ratios approximating the ratio released by conspecific females. The ratio between components was poorly represented, however, in the firing-rate output of uniglomerular MGC projection neurons (PNs). PN firing rate was mostly insensitive to the ratio between components, and individual PNs did not exhibit a preference for a particular ratio. Recording simultaneously from pairs of PNs in the same glomerulus, we found that the natural ratio between components elicited the most synchronous spikes, and altering the proportion of either component decreased the proportion of synchronous spikes. The degree of synchronous firing between PNs in the same glomerulus thus selectively encodes the natural ratio that most effectively evokes the natural behavioral response to pheromone.

Keywords

Olfaction; Neural coding; Glomerulus; Pheromone; Neural synchrony

Introduction

For most animals, survival and reproduction depend on the innate ability of sensory systems to recognize particular complex stimuli. That recognition of stimulus objects depends on the configuration of their components has been studied mainly in visual processing, whether for relatively simple configurations that signify prey (Ewert 1997) or the more complex arrangement of the features of a face (Rolls et al. 1994). It is recognized increasingly that olfaction also relies on similar mechanisms (Lei and Vickers 2008; Wilson and Sullivan

Corresponding author: Dr. Joshua Martin. jpmartin@case.edu, Phone: 216-368-2298, Fax: 216-368-4672.

2011). The olfactory stimuli released by potential mates, sources of food, appropriate places to raise offspring, and other important sources often take the form of mixtures of volatile organic compounds (VOCs) with a behavioral significance that is more than the sum of their parts (Jinks and Laing 2001; Riffell et al. 2009a, 2009b; Martin and Hildebrand 2010). Moreover, the efficacy of chemical communication often relies on the production, by a sender, of mixtures of VOCs with characteristic proportions components and corresponding selectivity for the natural proportions by a receiver (e.g. Visser and Avé 1978; Cardé and Minks 1995; Takken et al. 1997; Bruce et al. 2005; Silva et al. 2005; Tasin et al. 2006; Najar-Rodriguez et al. 2010; Cha et al. 2011). This phenomenon is thought to be a co-evolutionary adaptation between senders and receivers that improves the accuracy of communication; however, how proportionality is encoded in the brain of the receiver is still poorly understood.

Much of the existing model of mixture processing in olfaction is based on experiments using mixtures of a few VOCs, often in arbitrary combinations (Tabor et al. 2004; Carlsson et al. 2007; Silbering and Galizia 2007; Silbering et al. 2008; Deisig et al. 2006; Johnson et al. 2010; Olsen et al. 2010; Trona et al. 2010; Kuebler et al. 2011). In response to binary mixtures of VOCs, the spatial pattern of responses in the first olfactory center of insects (the antennal lobe, AL) and mammals (the olfactory bulb) changes smoothly with the ratio of the mixture components (Carlsson et al. 2007; Khan et al. 2008; Fernandez et al. 2009), and a selective response for a particular ratio was not reported in any of these studies. In one important exception, behavioral selectivity for a particular ratio of one component of a moth's host-plant scent to the whole is paralleled by the selective response of one glomerulus to that ratio (Najar-Rodriguez et al. 2010). Despite the ecological and behavioral importance of VOC mixtures with characteristic ratios, however, neural selectivity for a particular ratio of components in a mixture has been demonstrated only rarely, and details of a mechanism that facilitates the encoding of component ratios remain elusive. We propose that by using stimuli with innate behavioral significance and a method that allows for finer temporal analysis of glomerular output, a mechanism for directly encoding the ratio of components in mixture may be elucidated.

The proportions of components of the sex pheromones released by female moths have particular importance: fidelity between sender and receiver prevents interbreeding between closely-related species (Roelofs and Cardé 1977; Linn et al. 1988, 1991; Minks and Cardé 1988; Vickers et al. 1991; Anton et al. 1997). This system represents a form of innate object recognition in olfaction (Martin and Hildebrand 2010) and is favorable for investigation of how complex olfactory stimuli are encoded in the olfactory system of a receiver. In this study, we use a stimulus with known ecological and evolutionary significance to explore how the ratio of components in a mixture is encoded by the olfactory system of a male moth (*Manduca sexta*).

As a well-established animal model for olfactory studies, *M. sexta* has proved to be useful for investigations of the spatiotemporal coding of natural stimuli. We capitalize on features of the pheromone-processing system that make it an experimentally tractable model for encoding the proportions among components of an olfactory stimulus. Two components of the pheromone released by females, present in a 2:1 ratio, are necessary and sufficient to evoke pheromone-mediated source-oriented flight in males (Tumlinson et al. 1989). Two populations of pheromone-responsive olfactory receptor cells (ORCs) in the male's antennae each respond selectively to one of these components and terminate in one of a pair of large glomeruli of the macroglomerular complex (MGC) (Kaissling et al. 1989), a sex-pheromone-processing region found in the male ALs many moth species (Boeckh and Boeckh 1979; Matsumoto and Hildebrand 1981; Kanzaki and Shibuya 1983; Christensen

and Hildebrand 1987a). Projection neurons (PNs) arborizing in one of the MGC glomeruli receive excitatory input from the single population of ORCs terminating in that glomerulus. These PNs are also inhibited by local interneurons arborizing in both that glomerulus and the neighboring one in the MGC that is driven by the second population of pheromone-specific ORCs. The activity of PNs in either glomerulus thus is shaped by an excitatory response to one component and an inhibitory response to the other (Christensen and Hildebrand 1987b, Hansson et al. 1991, Heinbockel et al. 1999, 2004; Lei et al. 2002). Stimulation with both pheromone components at the natural ratio enhances the ability of the PNs to track discontinuous mixture stimuli and increases spiking synchrony between PNs in the same glomerulus (Lei et al. 2002).

We report here how the spiking output of the AL selectively encodes the behaviorally effective ratio of components in a natural stimulus across the distinct channels represented by glomeruli. Using stimuli matched between free-flight behavior in a wind tunnel and electrophysiological recordings of PNs in the AL of male *M. sexta*, we found that: (1) moths were selective for a range of mixture ratios surrounding the natural 2:1 ratio produced by females, and (2) pairs of PNs in the AL responded selectively to these ratios with enhanced spiking synchrony. Pheromone mixtures with altered ratios, created by increasing or decreasing either component, produced both reduced attraction to the source and reduced synchrony between spikes in the output of the MGC. We propose that the ratio coding discovered in this specialized, experimentally favorable system in an insect AL is also relevant to more general olfactory coding in insects and other taxa. Moreover, direct encoding of the configuration of a sensory object may be relevant to the processing of innate sensory stimuli in other modalities.

Materials and Methods

Preparation

Male *Manduca sexta* (Lepidoptera: Sphingidae) moths were raised in the laboratory on artificial diet (modified from that of Bell and Joachim 1976) under a long-day photoperiod (LD 17:7), as previously described (Sanes and Hildebrand 1976; Tolbert et al. 1983). Animals were prepared for physiological experiments as previously described (Christensen and Hildebrand 1987a). Moths were restrained with wax in a closely-fitting plastic tube. The labial palps and proboscis were removed, and a window was cut in the dorsal portion of the head capsule. The cibarial pump and other muscles were excised to allow access to the brain. One AL was desheathed to facilitate electrode penetration. To eliminate movement, the head was removed and pinned to a wax-coated petri dish, with the ALs oriented upward. The preparation was superfused with a saline solution (150 mM NaC1, 3 mM CaC12, 3 mM KC1, 10 mM TES buffer, and 25 mM sucrose, pH 6.9; Christensen and Hildebrand 1987b).

Behavioral experiments

Attraction to a mixture of pheromone components was investigated by use of a custom-made Plexiglas® wind tunnel (L × W × H = 4 × 1.5 × 1.5 m). Fans forced air through a series of filters and baffles into the tunnel, producing a uniform, unidirectional flow (wind speed 20 cm/s) that facilitates the formation of a plume of volatiles from a source to the end of the tunnel. The stimulus source was a 1-cm^2 piece of filter paper bearing 4 μl of one of the pheromone mixtures (see Table 1) or 4 μl of cyclohexane control centered vertically and laterally in the tunnel, 30 cm from the upwind vent. The concentration of pheromone components used in these experiments was chosen to approximate the rate of pheromone emission by a calling female moth (Lei et al. 2009).

A naïve male moth (2-3 days post-emergence) was placed on a platform 3.5 m downwind and allowed to respond for 5 min or until contact was made with the stimulus source. Moths that did not take flight within 5 min were not scored nor considered in the analysis. White and red low-intensity lights (0.5 lux) illuminated the tunnel and facilitated behavioral scoring and video recording of the flight paths. Video records were made on magnetic tape using a CCD video camera (Cohu model 6415-2000) with a macro lens and were used to confirm real-time behavioral scoring. The presence or absence of the following behaviors was recorded: upwind flight (within 1.5 m of the stimulus source), approach (flight directed toward the stimulus source, within 0.75 m), close hovering (cessation of forward movement and hovering within 10-30 cm of the stimulus source), contact with the source, and abdomen curl (a typical mating posture). Moths were tested in the second hour after the beginning of scotophase. Individual moths were tested with one of 5 stimulus mixtures, one of three dilutions of the 2:1 mixture, or cyclohexane control (Table 1). Stimulus samples were chosen semi-randomly for each trial. Overall stimulus effects and pair-wise comparisons between stimuli were tested using the chi-square and Fisher exact tests, respectively, with an alpha level of 0.05 (Sigma Plot 11, Systat Software, CA, USA).

EAG calibration of stimulus concentration

A battery-powered electroantennogram (EAG) device (PRG-2, Syntech, Hilversum, Netherlands) mounted on a stand was placed in the wind tunnel, centered vertically and laterally, 0.3 m from the stimulus source. Antennae were removed from male *M. sexta* (n=4) at 2-3 days post-emergence, and attached to the EAG probe using electrode gel (Spectra 360, Parker Laboratories Inc., NJ, USA). The antennae were rotated such that the ventral side faced upwind, toward the stimulus source. Signals were acquired via a PC interface board (IDAC-02, Syntech, Hilversum, Netherlands) and Autospike32 (Syntech) software in a notebook computer. EAG responses were identified as significant (>2 standard deviations) deflections from baseline using custom software in MATLAB (The MathWorks, Inc., Natick, MA, USA). The peak amplitudes of all detected EAG responses were measured from the baseline, and the mean, standard deviation, and range of all recorded deflections were calculated. The EAG device was inserted into the recording station used for the paired single-cell recordings (described below), and antennae from additional *M. sexta* males (n = 4) were stimulated with 15 pulses of each of 5 concentrations of the 2:1 pheromone mixture: 3000, 300, 30, 3, and 0.3 ng/μl total concentration. The amplitudes of the evoked EAG deflections were calculated as above.

Juxtacellular Recording

In order to record the responses of pairs of neurons to a large (10-15) battery of stimuli, the longer duration of recordings that is achievable with extracellular recording techniques was required. We therefore used a juxtacellular recording method adapted from Pinault (1996; Lei et al. 2009). This technique allows for high signal-to-noise ratio for the detection of spikes from a single cell and for recording sessions lasting several hours. Thin-wall borosilicate glass capillaries were pulled using a laser electrode puller (Sutter P-2000, Sutter Instrument Co., Novato, CA, USA) to a tip diameter of ca.1 μm. Electrodes were filled with a 2M KCl solution, yielding resistances <20 MΩ. Signals were amplified to 1,000× with an Axoprobe-1A amplifier (Axon Instruments, Union City, CA, USA) and an inline 10× DC amplifier (Model FC-23B, World Precision Instruments, Sarasota, FL). Two electrodes were inserted into the AL with Leica micro-manipulators (Leica Micro-Systems, Inc., Buffalo Grove, IL, USA) into the MGC region and advanced slowly until spikes were distinguishable from baseline noise. Only recordings with single spike amplitude (corresponding to spikes from a single cell) were retained for analysis.

Data acquisition and analysis

Analog recordings were digitized at 25 kHz using Datapak (Run Technologies, Mission Viejo, CA). All spiking data were processed and analyzed using custom MATLAB software (The MathWorks, Inc.). For each individual neuron, the timestamps of each spike were extracted, and a peri-stimulus time histogram and interspike-interval histogram were produced for each stimulus. From these, the peak firing rate, mean instantaneous firing rate, and interspike-interval variability (coefficient of variation) (Softky and Koch 1993) were calculated. For each paired recording, the shift-predictor-subtracted cross-correlogram and cross-interval histogram (Perkel et al. 1967a) were produced as measures of the synchronous firing of neurons. The shift-predictor accounts for chance coincidence of spikes by subtracting the average coincidence between spike trains in non-simultaneous trials, leaving the residual correlation attributable to physiological mechanisms of synchronization.

A correlation-based similarity metric was calculated as an additional measure of synchrony sensitive to fine-scale spike timing (Schreiber et al. 2003, Lyttle and Fellous 2011). The latter method confers several benefits over the more widely used histogram-based methods: it does not require the choice of an arbitrary bin size and performs better in discriminating between responses that vary only in the degree of synchronous firing (Paiva et al. 2010), and depending on the choice of kernel used in the method (see below), it can make predictions about characteristics of the cell decoding information contained in synchronous spikes (see Discussion). Briefly, spike trains are convolved with a kernel. Effectively, each spike train is represented as a time series the length of the trial.

A time-dependent function (the kernel) is inserted at each spike timestamp, decaying back towards zero between spikes. For this application, we have chosen a causal decaying exponential function $h(t) = \exp(-t/\tau)u(t)$, where $u(t)$ is the Heaviside step function, and τ is the time constant. This kernel is chosen to mimic the membrane properties of a coincidence detector and is more sensitive to small differences in synchronous firing (Paiva et al. 2010). The resulting convolved spike trains are represented as vectors for n neurons and i trials: $\overrightarrow{s_{n,1}}(i=1,\ldots N)$. A distance measure is used to calculate the similarity between simultaneously recorded spike trains. The inner product is taken between all paired spike trains for each trial and divided by the norms of each individual spike train in the trial. Similarity between simultaneously recorded spike trains 1 and 2 for trial i in response to a stimulus is therefore computed as:

$$S_i = \frac{\overrightarrow{S_{1,l}} \cdot \overrightarrow{S_{2,l}}}{\|\overrightarrow{S_{1,l}}\| \|\overrightarrow{S_{2,l}}\|}$$

The mean similarity is calculated across trials for each stimulus, and this is repeated for each of a series of time constants. The size of the time constant determines the rate of decay of the exponential kernel; therefore, smaller time constants result in a measure of similarity that is more sensitive to more precise synchrony between neurons. In analogy to the shift-predictor method for histograms, for each stimulus, neuron pair, and time constant, we calculate similarity between all non-simultaneous spike trains and subtract the mean of this value from the mean similarity between simultaneous pairs (Perkel et al. 1967b; Nowak et al. 1995; Kohn and Smith 2005). This provides a measure of “residual” similarity, i.e. the similarity that is greater than expected by chance coincidence in spike trains with a given firing rate and large-scale firing pattern.

For each response measure, we quantify selectivity for particular stimuli by computing the lifetime sparseness (*Sel*):

$$Sel = \frac{1 - [(\sum r_i/n)^2/(\sum r_i^2/n)]}{1 - (1/n)}$$

where r_i is the response to stimulus i and n is the number of stimuli in the series (Vinje and Gallant, 2000). This nonparametric statistic takes values between 0 (nonselective) and 1 (highly selective). For measures of synchrony, selectivity was calculated for each of a series of kernel decay constants used in calculating similarity. As the decay constant τ is comparable to bin width used in more traditional histogram methods (Kruskal et al. 2007), this facilitates a comparison of the selectivity of responses considering only spikes with a given degree of precision. For each stimulus series and response measure, we also tested overall stimulus effects and pairwise comparisons by a one-way repeated measures ANOVA and Fisher least-squares distance.

Sensory stimulation

Olfactory stimuli were delivered by injecting pulses of stimulus-laden air (250 ms duration, 0.1 l/min) into a constant clean air flow (1 l/min) directed at the middle of the antenna ipsilateral to the AL from which recordings were made. A solenoid-activated valve controlled by an electronic stimulator (World Precision Instruments) produced trains of 15 pulses at 250-ms intervals. Air from the valve was directed through a 0.5-ml glass syringe containing filter paper loaded with 1 μl of pheromone components diluted in cyclohexane. The stimuli consisted of two key pheromone components presented either alone or in mixtures: the major component (*E*,*Z*-10,12-hexadecadienal, BAL) and minor component (*E*,*E*,*Z*-10,12-14-hexadecatrienal, EEZ) of the female's sex pheromone (Tumlinson et al. 1989, 1994). The natural ratio of BAL to EEZ found in solvent washes of the female's pheromone gland is approximately 2:1 (Tumlinson et al. 1989). Additional mixtures used in the physiological experiments are presented in Table 2.

Characterization of neurons

The juxtacellular recording technique can allow for intracellular staining of neurons from which recordings have been made but with a low (<10%) success rate. Therefore, identification of uniglomerular MGC PNs (uPNs) and, especially, discrimination of these PNs from LNs and multi-glomerular PNs, relied on the physiological attributes of previously recorded and intracellularly stained PNs. We focused on MGC PNs that arborized in one of the two main glomeruli of the MGC, the cumulus or toroid I (Hansson et al. 1991). Three criteria were used: a bursting spontaneous firing pattern, response specificity to pheromone components, and a multi-phasic response pattern). ORCs that are highly selective for one of the two key components of the female pheromone (BAL or EEZ) confer their specificity to the PNs arborizing in that glomerulus (toroid I or cumulus, respectively) (Hansson et al. 1991; Heinbockel et al. 1999; Kalinova et al. 2001) such that PNs respond with excitation to only one component. Stimulation with the other key component of the pheromone activates ORCs that project to the neighboring glomerulus, where they synapse on LNs that feed forward to the PNs not directly excited by that component (Heinbockel et al. 1999). Uniglomerular MGC PNs thus are excited by stimulation with one component, inhibited by or unresponsive to the other component, and excited by a mixture of both components (Christensen and Hildebrand 1987b; Heinbockel et al. 1999, 2004; Lei et al. 2002). uPNs with dendrites in the cumulus respond with excitation to EEZ and inhibition of background

spiking or no response to BAL. Similarly, uPNs with dendrites in toroid I respond with excitation to BAL and inhibition of background spiking or no response to EEZ. Both types of PNs respond with excitation to mixtures of both components. Responses to the pheromone mixture are multi-phasic, with a brief period of inhibition (I_1), followed by a burst of spikes, and finally a longer period of after-hyperpolarization (I_2) before returning to a baseline firing rate (Christensen and Hildebrand 1987b). While I_1 is not visible in extracellular recordings, I_2 is reliably present and is used to characterize uPNs. Finally, the background firing pattern of MGC PNs is characterized by random bursts of spikes, while LNs exhibit more regular, constant background firing, and this trait can be used to discriminate reliably between cell types (Lei et al. 2011).

Results

Behavioral experiments

To begin the search for neural activity that encodes the proportions among components of a behaviorally significant stimulus mixture, we first determined whether *M. sexta* males exhibit innate selectivity for a particular ratio of the two key sex-pheromone components emitted by a conspecific female. Naïve male moths were tested individually in the wind tunnel (Fig. 1a) for attraction to pheromone mixtures, ranging from the natural 2:1 ratio (BAL:EEZ) emitted by female moths to mixtures with a 100-fold difference between components (Table 1). The ratio between components did not affect (Chi-square test, $P>0.05$) the percentage of males initiating upwind flight or the percentage that approached the pheromone source (Fig. 1b), indicating that detection and longer-range attraction were not influenced by this feature of the stimulus. For behavior close to the source, there was a significant relationship between the ratio of components and the percentage of males exhibiting both close hovering over the source (the filter paper emitting the stimulus mixture) and contact with it (Chi-square test, $P<0.05$). For these behaviors, only the 2:1 and 0.2:1 ratios were significantly different from control (cyclohexane, Fisher exact test $P<0.05$). In the final stages of a natural mating approach, the male adopts a mating posture with the abdomen curled under the female (in these experiments, the filter paper bearing the pheromone mixture). This behavior was significantly affected by the ratio of pheromone components (Chi-square test, $P<0.001$), and the natural 2:1 ratio as well as the 0.2:1 and 2:0.1 ratios were significantly different from control (Fisher exact test $P<0.001$ and $P<0.05$). These data demonstrate a behavioral selectivity for pheromone mixtures within one order of magnitude from the natural 2:1 ratio emitted by females.

To control for the decrease in total concentration effected by changing the ratio of pheromone components, we performed additional experiments testing animals with serial dilutions of the 2:1 ratio mixture. Total concentration did not significantly affect the percentage of males exhibiting all scored behaviors (Fig. 1c, close hovering and abdomen curling shown, Chi-square test, $P>0.05$), and behavior was significantly different from control at all concentrations (Fisher exact test, $P<0.05$).

Electrophysiological experiments

Having demonstrated behavioral selectivity for a range of ratios of pheromone components centered on the natural 2:1 ratio produced by female moths, we next examined how varying the ratio of the two key components influenced the neural representations of these mixtures in the AL. First, we calibrated the stimuli delivered in the electrophysiological experiments to correspond to the intensity of stimuli encountered in the behavioral experiments. Electroantennogram (EAG) recordings in the wind tunnel, taken at a distance from the source where both “approach” and “close hovering” behaviors were observed, revealed a

highly variable response of the male antenna (mean amplitude of 0.09 mV, range from 0.015 to 0.33 mV; 0.82 ± 0.22 deflections/second, mean ± SD, measured valley to valley; n = 10 antennae) (Fig. 1d). In analogous recordings in the electrophysiological recording station used for the following experiments, all but the highest concentration of the 2:1 ratio mixture (0.3, 3, 30, 300, and 3000 ng/μl) produced EAG deflections within the range observed in the wind tunnel (0.057 ± 0.016 mV, 0.086±0.047 mV, 0.107±0.097 mV, 0.209±0.097 mV, 0.604±0.224 mV, mean ± SD) (Fig. 1d). The intensities of stimuli used in the electrophysiological experiments therefore were considered to be comparable to those used in the behavioral experiments.

We obtained 19 simultaneous paired recordings from uniglomerular PNs that arborized in one of the two main glomeruli of the MGC (the cumulus or toroid I). These neurons typically exhibited a pattern of background firing characterized by bursts, a triphasic response to olfactory stimulation, and excitation to one component of the mixture and inhibition or no response to the other component (see Materials and Methods). We used this response profile to recognize uniglomerular MGC PNs. For simplicity, we refer to PNs that arborized in the cumulus and responded with excitation to EEZ as ‘EEZ -PNs’ and PNs that arborized in toroid I and responded with excitation to BAL as ‘BAL-PNs.’ Of the 19 pairs of PNs in these experiments, 13 were pairs of EEZ-PNs, 2 were pairs of BAL-PNs, and 4 were mixed EEZ-PN/BAL-PN pairs. The EEZ-PN/BAL-PN pairs did not exhibit significant spiking synchrony in response to pheromonal stimuli (Lei et al. 2002) and hence were not included among the examples analyzed here. While both EEZ- and BAL-PN pairs exhibited similar responses in all experiments, the low number of BAL-PNs prohibited analysis of each population separately. Inclusion of the minority BAL-PN pairs did not affect the results of analysis of the 13 pairs of EEZ-PNs alone. Therefore, the results presented below incorporate both BAL- and EEZ-PN pairs.

Hereinafter, we refer to the component that elicits a spiking response in a cell as the “excitatory component” and the component that produces suppression of spiking or no response as the “inhibitory component.” This distinction is purely from the perspective of a single neuron in a particular glomerulus and does not imply a behavioral consequence.

Responses of individual PNs

In all recorded individual neurons, stimulation with mixtures containing increasing concentrations of the excitatory component mixed with a single concentration of the inhibitory component produced responses with decreasing latency and increasing spiking frequency (see Fig. 2a, top panel for example). This concentration-dependent response was similar to responses to stimulation with increasing concentration of the excitatory component alone (Fig. 2b). For both series, responses saturated such that the three highest concentrations evoked statistically indistinguishable responses in BAL-PNs and EEZ-PNs (Tukey test, $P<0.05$). Response variability across all recorded neurons, however, was generally reduced in the responses to the mixtures and was significantly reduced at the 2:1 ratio (Levene's test, $P<0.05$). Thus the presence of the inhibitory component in the mixture reduced the variability of response firing rate in a ratio-dependent manner.

Mixtures with varying concentrations of the inhibitory component elicited responses with similar time course and peak firing rate (see Fig. 2a, bottom panel for example). Varying the relative proportion of the inhibitory component did not significantly alter the mean firing rate across all recorded neurons (Fig. 2c, thick lines, Friedman repeated measures ANOVA, $P>0.05$) or the temporal features of responses of individual cells (Fig. 2c, gray lines). This is consistent with previous observations that the inhibitory connection between MGC

glomeruli does not simply decrease firing rate (Waldrop et al. 1987; Christensen and Hildebrand 1997; Heinbockel et al. 1999; Lei et al. 2002).

Finally, we tested the hypothesis that the ratio between components might be encoded in the relative firing rate between PNs responding to each component. For this, we randomly paired neurons and calculated the ratio between the mean instantaneous firing rates of each cell in response to different concentrations of the cell's excitatory component. The result is a shallow curve that, while generally increasing with the ratio between components, exhibits no statistically different responses at any ratio (Fig. 2d, Friedman repeated measures ANOVA, $P>0.05$). This reflects both the variability and saturation of individual responses to concentrations of an individual component. Thus while some information about the ratio between components is available in the relative responses of individual PNs, the signal-to-noise level of this representation is quite low.

Synchrony in PN pairs

As spiking synchrony between PNs in the MGC has been demonstrated previously to depend on the presence of both key components of the pheromone mixture, we next tested whether the degree of synchrony may further encode the ratio between components in the mixture. To quantify spiking synchrony, we used both the cross-interval histogram (Perkel et al. 1967b), which reports the probability of observing spikes in two cells with a particular latency, and a “binless” method that computes the similarity between spike trains using a correlation-based metric (Schreiber et al. 2003). An example of these measures for a pair of MGC PNs is shown in Fig. 3, panels c and d. Although the results displayed in this example are from an experiment in which the inhibitory component (BAL) was varied and the excitatory component (EEZ) held constant, similar results were obtained from a corresponding series in which the excitatory component was varied, and in the population data (Fig. 4) we report results from both experiments.

The cross-interval histogram for the example pair revealed a greater proportion of spikes with intervals between 0 and 4 ms for all mixtures compared to the excitatory component presented alone (Fig. 3a and b). The ratio between components in the mixture affected chiefly the proportion of spikes with intervals between 0 and 2 ms, with the greatest proportion of spikes in these intervals observed in response to the natural 2:1 mixture. The binless method revealed a similar effect of component ratio on similarity between simultaneously recorded spike trains from this example pair (Fig. 3c,d). For both methods, we used a shift-predictor-subtraction method (Perkel et al. 1967b) wherein the average synchrony between non-simultaneous responses provided an estimate the coincidence between spikes expected by chance, i.e. attributable to factors such as the firing rate of each cell. Subtracting this expected coincidence from the observed coincidence between simultaneously recorded spike trains yielded a measure of the synchrony generated by the activity of the neural circuitry not attributable to chance (see Materials and Methods). For the example pair in Fig. 3, both analyses revealed greater shift-predictor-subtracted synchrony in response to the 2:1 mixture than to other mixtures (Fig. 3b, d). The binless method, however, allows a finer scale of analysis and revealed a peak in shift-predictor-subtracted synchrony at a particular kernel size (the width of the function convolved with the spike trains, comparable to the interval in the cross-interval histogram) for each mixture. Therefore, results were comparable for both measures of spiking synchrony.

We proceeded to use the shift-predictor-subtracted similarity as our measure of synchronous firing between pairs of neurons and next analyzed the representation of the ratio between components of the pheromone using this measure. For each kernel size (i.e. for synchronous spikes with a particular degree of precision), the synchrony-based selectivity was calculated

as a measure of the "tuning" of the pair of neurons to a particular ratio between components (Fig. 3f). Of 19 pairs of PNs recorded, 12 exhibited a peak in selectivity at a particular kernel size for stimuli in which the proportion of either the excitatory or inhibitory component was manipulated. The majority (10 out of 12) of PN pairs exhibited a peak in selectivity for a particular ratio between 0 and 5 ms. The position of this peak was variable but most commonly was found between 0 and 1 ms (Fig. 3f). Of the 10 pairs that were tested with both manipulations, eight pairs exhibited selectivity for a particular ratio when either the excitatory or inhibitory component was altered. For the remaining two pairs, a peak in selectivity was observed only when the excitatory component was altered. Fig. 3e illustrates the tuning of a PN pair's response to particular ratios of the pheromone components at kernel widths for the peak (black line) and minimum (grey line) selectivity.

Although 8 out of 12 pairs had maximal shift-subtracted synchrony in response to the natural 2:1 ratio, other pairs exhibited tuning to mixtures with other proportions of either the excitatory or the inhibitory component. For both manipulations, averaging across all selective pairs yielded a population tuning curve with a peak at the natural 2:1 ratio. Although we recorded from pairs of neurons mainly in one glomerulus (the cumulus), we assume that synchrony-based tuning operates simultaneously in both responding glomeruli, i.e. as PNs in one MGC glomerulus respond to mixtures with varying proportions of their cognate excitatory component, at the same time PNs in the neighboring glomerulus respond to mixtures with varying proportions of their inhibitory component. Indeed, mixtures with varying proportions of either BAL or EEZ produced maximally synchronous activity in the population of recorded cells at the natural 2:1 ratio (Fig. 4a,b). There was a significant interaction between component ratio and shift-predictor-subtracted similarity for both sets (one-way repeated measures ANOVA, $P<0.05$). In parallel with the behavioral data, the 2:1 ratio was significantly different from all but the neighboring ratios (Fisher's least significant difference, $\alpha = 0.05$). The neural selectivity represented by shift-predictor-subtracted similarity was not correlated with the behavioral selectivity exhibited by males in performing either of the two long-distance flight behaviors (Pearson's coefficient: upwind flight, $R = 0.47$, and approach, $R = 0.42$, $P>0.05$) but was strongly correlated with the three near-distance flight and mating behaviors (Pearson's coefficient: close hover, $R = 0.88$, contact, $R = 0.97$, and abdomen curling, $R = 0.97$, $P<0.05$). We therefore conclude that increased spiking synchrony, as measured by shift-predictor-subtracted similarity, constitutes a representation of the ratio between components of the pheromone mixture. Furthermore, the ratio is represented not as an absolute value but relative to the 2:1 ratio released by female moths and most attractive to males.

Discussion

Recognizing behaviorally relevant VOC mixtures based on the configuration of their components is likely common among diverse animal species, but it is challenging to explain this capacity with the current models of olfactory information processing. Examples include the remarkable ability of rodents to identify individuals and hymenopterans to identify nestmates through "signature mixtures" of common VOCs released in characteristic proportions (see Wyatt 2010 for review). The well-established combinatorial coding hypothesis (Xu et al. 2000; Leon and Johnson 2006; Koulakov et al. 2007; Galizia and Szyszka 2008) may explain how qualitatively different olfactory stimuli are represented in the olfactory bulb or AL, but perhaps not the quantitative relationships critical to the salience or behavioral significance of a particular mixture, as the same set of glomeruli can be activated by similar mixtures that have very different behavioral significance (c.f. Brandstaetter et al. 2011). These higher-order features of "odor objects" may be encoded on

the basis of higher-order features of the population code such as the degree of spiking synchrony among particular central neurons.

In this study we have demonstrated that the degree of synchronous activity between PNs associated with the same glomerulus in the AL of *M. sexta* encodes the natural, behaviorally effective ratio between two key components (BAL and EEZ) of the sex-pheromone mixture of this species. In behavioral tests using pheromone lures with various ratios of these components, male moths exhibited increasingly complete behavioral responses as mixtures approached the natural 2:1 ratio and ultimately adopted the typical mating posture (abdomen curling) as they approached a lure emitting that natural ratio. Both the mean instantaneous firing rates of individual PNs in the AL and the ratio between the firing rates of PNs responding to different concentrations of each component were largely insensitive to component ratios. However, synchronous spiking between pairs of PNs in the same glomerulus was increased for ratios in a range of plus or minus 1 order of magnitude surrounding the natural 2:1 ratio. Individual pairs of neurons were selective for a particular ratio in this range, and all selective pairs showed reduced selectivity to higher or lower ratios and to the individual components alone. This finding of ratio-coding neural mechanisms in *M. sexta* may have broad behavioral and ecological relevance for other species.

Male M. sexta exhibit selectivity for the natural component ratio at close range

Many moth species are sympatric with closely related species that employ the same pheromone components for male-female communication, differing only in the mixture proportions produced by females and attractive to males (Minks et al. 1973; Löfstedt et al. 1991; Dunkelblum and Mazor 1993; Schlyter et al. 2001; Ming et al. 2007; Yang et al. 2009). Although the composition of sex pheromones released by other sympatric species of *Manduca* have not yet been described, the behavioral selectivity for the natural 2:1 ratio between the BAL and EEZ components we observed in our wind tunnel tests (Fig. 1b) is similar to the selectivity determined in wind-tunnel and field-trapping studies with other moth taxa (see Schlyter et al. 2001). The range of acceptable pheromone ratios, or the "response window" (Roelofs 1978), in *M. sexta* was considerably wider than that found for many other moths but was comparable to the response window for *Agrotis segetum* (Löfstedt et al. 1985) and species of the genus *Adoxophyes* (Yang et al. 2009).

The selectivity of male *M. sexta* for the 2:1 ratio of pheromone components increased for behaviors exhibited nearer the stimulus source (Fig. 1b). Similar sharpening of the behavioral response has been observed for corresponding behavioral steps in other moth species (Baker et al. 1981; Linn and Roelofs 1983; Linn and Roelofs 1985; Schlyter et al. 2001). There was no significant difference between ratios in eliciting upwind flight toward the lure, and little difference in eliciting an approach to the lure, suggesting that the presence of pheromone components, regardless of their proportions in the mixture emitted by a lure, exceeds the "orientation threshold" for olfaction-mediated flight, and the abrupt change in behavioral selectivity between the "approach" and "close hovering" steps suggests that the ratio between components determines an "arrestment threshold" at this point (Roelofs 1978). Whether these changes in behavioral sensitivity reflect broader neural selectivity at a distance, or if the mechanism described here requires closer proximity to the lure, is not yet clear.

A large proportion of moths exhibited distant orientation behaviors (upwind flight and approach) to both "off" mixtures and the solvent control. Several other authors utilizing solvent control report similar responses in *M. sexta* (Lei et al. 2009; Tumlinson et al. 1989) and other species (El-Sayed et al. 1999), while others report no upwind flight to solvent (c.f. Baker and Cardé 1979). Initiation of flight and upwind flight under these experimental

conditions may be attributable to purely mechanosensory input in these animals (Budick et al. 2007; Sane et al 2007). A large number of reports, however, do not report solvent control, but report zero or near-zero initiation of flight, upwind flight, or both to “off” pheromone mixtures (c.f. Willis and Baker 1988; Roelofs 1978; Baker et al. 1981; Linn and Roelofs 1983). These differences may be attributable to the inhibition of flight by an “off” mixture. Others report a non-selective response similar to that reported here for behaviors distant from the source (Baker et al. 1981; Quero and Baker 1999; Schlyter et al. 2001). While comparisons between studies cannot rule out differences attributable to experimental design, these differences may reflect variation across species in stimuli that induce a distant response.

Firing rates of individual PNs are mostly insensitive to ratio

We tested two hypotheses about the firing rates of responses of MGC PNs: (1) the ratio between components in the mixture is represented by a ratio-dependent modulation of PN firing rate, such that output is maximal at the behaviorally effective ratio of stimulus components (as observed in Najar-Rodriguez et al. (2010) for host-plant VOCs); and (2) the concentration-dependent responses of individual PNs form the basis of a ratio code that is read out at higher levels of processing, i.e. the ratio of components is reflected in the ratio between firing rates of PNs in each MGC glomerulus. Pheromone-responsive MGC PNs encode in their firing rates the concentration of the component to which they are selective (Kanzaki et al. 1989; Christensen et al. 1991; Hartlieb et al. 1997; Jarriault et al. 2009) (Fig. 2b). When combined with a constant concentration of the inhibitory component, so as to generate a series of component ratios (Table 2), we observed no selective, increased response to a particular ratio (Fig. 2b). As our primary interest is in how communication between separate output channels (i.e. uniglomerular PNs (uPNs) in each glomerulus) contribute to encoding the ratio between components, we did not examine multi-glomerular PNs (mPNs) that arborize in both MGC glomeruli in this study. mPNs have been observed occasionally to exhibit mixture-specific responses (Hansson et al. 1991; Hansson et al. 1994; Christensen et al. 1995) and in a few recorded instances, to discriminate between component ratios of closely related species (Wu et al. 1996; Anton et al. 1997). These examples of a firing-rate-based code for mixture ratios may represent an additional, parallel channel, projecting along a separate anatomical tract from the AL (Galizia and Roessler 2010).

PN firing rates also were unaffected by the relative concentration of the inhibitory component in the mixture and showed neither inhibition of the response to the excitatory component nor a selective response for a particular ratio between components (Fig. 2c). Although communication between glomeruli is GABAergic and hyperpolarizing, inhibition in the MGC does not typically result in a reduction in PN firing rate when concurrent with excitatory input (Waldrop et al. 1987; Christensen and Hildebrand 1997; Heinbockel et al. 1999; Lei et al. 2002).

Although the firing rates of individual MGC PNs were not particularly sensitive to the ratio of pheromone components, ratio information could be encoded in the relative activity of PNs, in neighboring glomeruli, that encode the concentration of their respective excitatory components. Two observations make this coding scheme less likely, however. First, as the concentration of the excitatory component increased over four orders of magnitude, the average PN firing rate increased by only a factor of four, and the variability at each concentration could be 50% or more of the mean (Fig. 2b). Second, responses saturated (Fig. 2b) within the range of concentrations encountered in the behavioral experiments (Fig. 1d). While the ratio between pairs of PN responses to different concentrations of their excitatory components (recorded non-simultaneously) generally increased with greater difference between component concentrations, the range of firing rate ratios was small and nearly

entirely encompassed by the variability at any one component ratio (Fig. 2d). Most importantly, firing rate ratios in response to component ratios that were behaviorally "rejected" (i.e. behavioral responses were indistinguishable from control) were not significantly different from those in response to attractive component ratios. We conclude that while some information about component ratio is available in this dimension of the output, it is not selective for behaviorally effective ratios. However, a variety of mechanisms may account for behaviors selective for particular configurations of complex odors, (Lei and Vickers 2008; Clifford and Riffell 2013), and may indeed operate in parallel. In the pheromone system of *Helicoverpa zea*, a purely combinatorial code has been proposed, wherein an "antagonistic" glomerulus is activated at higher, unattractive concentrations of one component in the mixture (Vickers et al. 1998). Currently, we have no evidence of any glomerulus in the antennal lobe of *M. sexta* that would correspond to this "antagonistic" glomerulus in *H. zea*. Moths exhibit diverse patterns of attractive and repulsive pheromone component configurations (reviewed in Martin and Hildebrand 2010), and certainly other mechanisms may encode those patterns.

Processing at higher-order olfactory neuropil (e.g. the mushroom bodies or protocerebrum) may also produce selective output from less-selective input (c.f. Szyszka et al. 2005). Regions of overlap between PNs from each of the two main MGC glomeruli may be particularly sensitive to a code based on differences in firing rate (Homberg et al. 1988; Kanzaki et al. 2003; Seki et al. 2005). Finally, as diverse species of moths exhibit broad or narrow selectivity for pheromone component ratios (Schlyter et al. 2001), reliance on a particular encoding dimension (frequency or synchrony) may similarly vary. We would predict, however, that a species that relied on frequency encoding would (1) not exhibit saturation of firing rate output in the range of concentrations naturally encountered, and (2) exhibit little variability, i.e. more precision, in encoding the concentration of each component in the firing rate of the PNs in each glomerulus.

Enhancement of synchronous firing of PNs is selective for behaviorally effective ratios

An earlier study revealed that more synchronous spikes were produced by pairs of PNs in the same glomerulus in response to the 2:1 mixture of pheromone components than to the excitatory component alone (Lei et al. 2002). Several other studies also showed that synchrony between output neurons of the same glomerulus (Puopolo and Belluzzi 2001; Schoppa and Westbrook 2001; Lei et al. 2002; Kazama and Wilson 2009) or different glomeruli (Kashiwadani et al. 1999; Lei et al. 2004; Schoppa 2006a,b; Riffell et al. 2009a,b) is a common feature of olfactory processing in the AL and olfactory bulb. None of those studies, however, systematically changed the component ratios during testing. In our work, we found that pairs of MGC PNs exhibited maximal shift-predictor-subtracted synchrony to pheromone mixtures with component ratios near the natural 2:1 ratio (Fig. 4). In most pairs recorded, selectivity for a particular ratio was maximal for synchronous spikes within 1-5 ms (Fig. 3f). This high degree of precision is comparable to the "sharpest" synchrony observed in the mammalian brain (Mastronarde 1983; Alonso et al. 1996; Swadlow et al. 1998; Schnitzer and Meister 2003; Takahashi and Sakurai 2009).

The firing rates of individual PNs in an MGC glomerulus reflect the concentration of their excitatory component, while the degree of synchronous activity between pairs of PNs in the same glomerulus reflects the ratio between components in the mixture. In effect, firing rate and synchrony are separate output channels carrying different information to higher-order centers in the brain. This finding parallels results in the olfactory system (Christensen et al. 1998; Friedrich et al. 2004) and other systems (deCharms and Merzenich 1996; Meister 1996; Riehle et al. 1997; Dan et al. 1998; Biederlack et al. 2006) and supports the concept of "multiplexed coding" in sensory systems (Panzeri et al. 2010). As complex, natural olfactory

stimuli can be characterized by dimensions including the identity of the components, their individual concentrations, and the relative proportions among them, so can the activity or silence of PNs, their firing rates, and the synchronous activity among them provide semi-independent dimensions for encoding information about an olfactory stimulus.

Enhanced synchronous firing between PNs in the moth's MGC encodes information about the relationship between features of a stimulus mixture and thus resembles the “binding” of features of visual objects by the synchronous activity between channels responding to each feature (Singer 1999). Our results, however, and those presented earlier (Lei et al. 2002) differ from the standard model of binding in that synchronous activity of neurons within a channel, instead of across channels, encodes information about the configuration of features in the stimulus object.

While our results demonstrate that MGC PNs encode the pheromone component ratio in the degree of synchronous output, details of the production and reception of this output remain to be investigated. Previous work demonstrated that the degree of synchrony between MGC PNS in one glomerulus in response to the natural pheromone mixture was dependent on inhibition from LNs driven by input to the neighboring MGC glomerulus (Christensen et al. 2003; Lei et al. 2002). Synchronization of AL output by inhibition is a common feature of insect olfactory systems (reviewed in Martin et al. 2011). Genetic alteration of interglomerular inhibition has been proposed as a mechanism in the evolution of groups of related moth species that utilize different ratios of the same pheromone components (Baker 2008). A recent model of a moth MGC proposed that ratio-selective PN output can be produced by an as-yet-undiscovered inhibitory network that generates a ratio-dependent inhibitory input to MGC PNs (Zavada et al. 2011). While this model proposed a firing-rate code for component ratios, it could possibly be modified to generate a synchrony-based ratio code.

Finally, the coincident arrival of synchronous spikes is generally more effective at depolarizing membranes through near-linear or even supralinear temporal summation (Magee 2000). Therefore, the PN output in response to the behaviorally effective blend ratio may more readily activate higher-order olfactory centers. The finding of a synchrony-based code for the observed ratio-selective behavior, however, suggests that coincidence-detecting neurons such as those described in the mushroom body (Perez-Orive et al. 2002, 2004) may be found: cells with rapid membrane dynamics could respond selectively to the increased synchrony PN output representing the natural blend. In an accompanying report (Lei et al., this issue), we describe cells in the protocerebrum that respond selectively to ratios in the behaviorally effective range.

We have demonstrated that the output of the AL of male *M. sexta* encodes the behaviorally effective ratio between key pheromone components in the degree of synchronous firing of PNs in the MGC. This work confirms and expands upon our previous finding that synchrony of PN spiking in the AL encodes the behavioral significance of olfactory stimuli (Lei et al. 2002; Riffell et al. 2009b; Martin and Hildebrand 2010). Furthermore, this work adds to the growing understanding (Atick 1992; Dusenberry 1992; Rieke et al. 1995; Machens et al. 2001; Yu et al. 2005; Garcia-Lazaro et al. 2006) that neural circuits are adapted to the structure of stimuli important to an animal's survival and reproduction.

Acknowledgments

The authors would like to thank E. Constantopoulos for assistance with behavioral experiments, and A. M. Dacks, C. E. Reisenman, A. Beyerlein, and J. M. Fellous for helpful discussion and comments on this work. This research

was supported by the National Institute on Deafness and Other Communication Disorders (NIDCD) grants RO1-DC02751 to JGH and NRSA DC97222 to JPM.

References

Alonso JM, Usrey WM, Reid RC. Precisely correlated firing in cells of the lateral geniculate nucleus. Nature. 1996; 383:815–819. [PubMed: 8893005]

Anton S, Löfstedt C, Hansson BS. Central nervous processing of sex pheromones in two strains of the European corn borer *Ostrinia nubilalis* (Lepidoptera: Pyralidae). J Exp Biol. 1997; 200:1073–1087. [PubMed: 9318892]

Atick JJ. Could information theory provide an ecological theory of sensory processing? Network: Comput Neural Syst. 1992; 3:213–251.

Baker TC. Balanced olfactory antagonism as a concept for understanding evolutionary shifts in moth sex pheromone blends. J Chem Ecol. 2008; 34:971–981. [PubMed: 18452043]

Baker TC, Cardé RT. Analysis of pheromone-mediated behaviors in male *Grapholitha molesta*, the oriental fruit moth (Lepidoptera: Tortricidae). Environ Entomol. 1979; 8:956–968.

Baker TC, Meyer W, Roelofs WL. Sex pheromone dosage and blend specificity of response by oriental fruit moth males. Entomol Exp Appl. 1981; 30:269–279.

Bell RA, Joachim FG. Techniques for rearing laboratory colonies of tobacco hornworms and pink bollworms (Lepidoptera-Sphingidae-Gelechiidae). Ann Entomol Soc Am. 1976; 69:365–373.

Biederlack J, Castelo-Branco M, Neuenschwander S, Wheeler DW, Singer W, Nikolic D. Brightness induction: Rate enhancement and neuronal synchronization as complementary codes. Neuron. 2006; 52:1073–1083. [PubMed: 17178409]

Boeckh J, Boeckh V. Threshold and odor specificity of pheromone-sensitive neurons in the deutocerebrum of *Antheraea pernyi* and *Antheraea polyphemus* (Saturnidae). J Comp Physiol A. 1979; 132:235–242.

Brandstaetter AS, Roessler W, Kleineidam CJ. Friends and foes from an ant brain's point of view - neuronal correlates of colony odors in a social insect. PLoS ONE. 2011; 6

Bruce TJA, Wadhams LJ, Woodcock CM. Insect host location: a volatile situation. Trends Plant Sci. 2005; 10:269–274. [PubMed: 15949760]

Budick SA, Reiser MB, Dickinson MH. The role of visual and mechanosensory cues in structuring forward flight in Drosophila melanogaster. J Exp Biol. 2007; 210:4092–4103. [PubMed: 18025010]

Cardé RT, Minks AK. Control of moth pests by mating disruption - Successes and constraints. Annu Rev Entomol. 1995; 40:559–585.

Carlsson MA, Chong KY, Daniels W, Hansson BS, Pearce TC. Component information is preserved in glomerular responses to binary odor mixtures in the moth *Spodoptera littoralis*. Chem Senses. 2007; 32:433–443. [PubMed: 17400588]

Cha DH, Linn CE, Teal PEA, Zhang AJ, Roelofs WL, Loeb GM. Eavesdropping on plant volatiles by a specialist moth: Significance of ratio and concentration. PLoS ONE. 2011; 6:8.

Christensen TA, Hildebrand JG. Male-specific, sex pheromone-selective projection neurons in the antennal lobes of the moth *Manduca sexta*. J Comp Physiol A. 1987a; 160:553–569. [PubMed: 3612589]

Christensen TA, Hildebrand JG. Pheromonal information coding by projection neurons in the antennal lobes of the sphinx moth *Manduca sexta*. Ann N Y Acad Sci. 1987b; 510:224–226.

Christensen TA, Hildebrand JG. Coincident stimulation with pheromone components improves temporal pattern resolution in central olfactory neurons. J Neurophysiol. 1997; 77:775–781. [PubMed: 9065849]

Christensen TA, Itagaki H, Teal PEA, Jasensky RD, Tumlinson JH, Hildebrand JG. Innervation and neural regulation of the sex-pheromone gland in female *Heliothis* moths. Proc Natl Acad Sci USA. 1991; 88:4971–4975. [PubMed: 2052579]

Christensen TA, Lei H, Hildebrand JG. Coordination of central odor representations through transient non-oscillatory synchronization of glomerular output neurons. Proc Natl Acad Sci USA. 2003; 100:11076–11081. [PubMed: 12960372]

Christensen TA, Mustaparta H, Hildebrand JG. Chemical communication in heliothine moths .6. Parallel pathways for information-processing in the macroglomerular complex of the male tobacco budworm moth *Heliothis virescens*. J Comp Physiol A. 1995; 177:545–557.

Christensen TA, Pawlowski VM, Lei H, Hildebrand JG. Multi-unit recordings reveal context-dependent modulation of synchrony in odor-specific neural ensembles. Nat Neurosci. 2000; 3:927–931. [PubMed: 10966624]

Christensen TA, Waldrop BR, Hildebrand JG. Multitasking in the olfactory system: Context-dependent responses to odors reveal dual GABA-regulated coding mechanisms in single olfactory projection neurons. J Neurosci. 1998; 18:5999–6008. [PubMed: 9671685]

Clifford MR, Riffell JA. Mixture and odorant processing in the olfactory systems of insects: a comparative perspective. J Comp Physiol A. 201310.1007/s00359-013-0818-6

Dan Y, Alonso JM, Usrey WM, Reid RC. Coding of visual information by precisely correlated spikes in the lateral geniculate nucleus. Nat Neurosci. 1998; 1:501–507. [PubMed: 10196548]

deCharms RC, Merzenich MM. Primary cortical representation of sounds by the coordination of action-potential timing. Nature. 1996; 381:610–613. [PubMed: 8637597]

Deisig N, Giurfa M, Lachnit H, Sandoz JC. Neural representation of olfactory mixtures in the honeybee antennal lobe. Eur J Neurosci. 2006; 24:1161–1174. [PubMed: 16930442]

Dunkelblum E, Mazor M. Chemical characterization and species specificity of sex-pheromones of plusiinae moths in Israel. Arch Insect Biochem Physiol. 1993; 22:413–424.

Dusenberry, DB. Sensory ecology: how animals acquire and respond to information. Freeman; New York: 1992.

El-Sayed A, Bengtsson M, Rauscher S, Lofqvist J, Witzgall P. Multicomponent sex pheromone in codling moth (Lepidoptera: Tortricidae). Environ Entomol. 1999; 28:775–779.

Ewert JP. Neural correlates of key stimulus and releasing mechanism: a case study and two concepts. Trends Neurosci. 1997; 20:332–339. [PubMed: 9246720]

Fernandez PC, Locatelli FF, Person-Rennell N, Deleo G, Smith BH. Associative conditioning tunes transient dynamics of early olfactory processing. J Neurosci. 2009; 29:10191–10202. [PubMed: 19692594]

Friedrich RW, Habermann CJ, Laurent G. Multiplexing using synchrony in the zebrafish olfactory bulb. Nat Neurosci. 2004; 7:862–871. [PubMed: 15273692]

Galizia CG, Roessler W. Parallel olfactory systems in insects: anatomy and function. Annu Rev Entomol. 2010; 55:399–420. [PubMed: 19737085]

Galizia CG, Szyszka P. Olfactory coding in the insect brain: molecular receptive ranges, spatial and temporal coding. Entomol Exp Appl. 2008; 128:81–92.

Garcia-Lazaro JA, Ahmed B, Schnupp JWH. Tuning to natural stimulus dynamics in primary auditory cortex. Curr Biol. 2006; 16:264–271. [PubMed: 16461279]

Hansson BS, Christensen TA, Hildebrand JG. Functionally distinct subdivisions of the macroglomerular complex in the antennal lobe of the male sphinx moth *Manduca sexta*. J Comp Neurol. 1991; 312:264–278. [PubMed: 1748732]

Hansson BS, Anton S, Christensen TA. Structure and function of antennal lobe neurons in the male turnip moth, *Agrotis segetum* (Lepidoptera: Noctuidae). J Comp Physiol A. 1994; 175:547–562.

Hartlieb E, Anton S, Hansson BS. Dose-dependent response characteristics of antennal lobe neurons in the male moth *Agrotis segetum* (Lepidoptera: Noctuidae). J Comp Physiol A. 1997; 181:469–476.

Heinbockel T, Christensen TA, Hildebrand JG. Temporal tuning of odor responses in pheromone-responsive projection neurons in the brain of the sphinx moth *Manduca sexta*. J Comp Neurol. 1999; 409:1–12. [PubMed: 10363707]

Heinbockel T, Christensen TA, Hildebrand JG. Representation of binary pheromone blends by glomerulus-specific olfactory projection neurons. J Comp Physiol A. 2004; 190:1023–1037.

Homberg U, Montague RA, Hildebrand JG. Anatomy of antenno-cerebral pathways in the brain of the sphinx moth *Manduca sexta*. Cell Tissue Res. 1988; 254:255–281. [PubMed: 3197087]

Jarriault D, Gadenne C, Rospars JP, Anton S. Quantitative analysis of sex-pheromone coding in the antennal lobe of the moth *Agrotis ipsilon*: a tool to study network plasticity. J Exp Biol. 2009; 212:1191–1201. [PubMed: 19329752]

Jinks A, Laing DG. The analysis of odor mixtures by humans: evidence for a configurational process. Physiol Behav. 2001; 72:51–63. [PubMed: 11239981]

Johnson BA, Ong J, Leon M. Glomerular activity patterns evoked by natural odor objects in the rat olfactory bulb are related to 14 patterns evoked by major odorant components. J Comp Neurol. 2010; 518:1542–1555. [PubMed: 20187145]

Kaissling KE, Hildebrand JG, Tumlinson JH. Pheromone receptor-cells in the male moth *Manduca sexta*. Arch Insect Biochem Physiol. 1989; 10:273–279.

Kalinova B, Hoskovec M, Liblikas I, Unelius CR, Hansson BS. Detection of sex pheromone components in *Manduca sexta* (L.). Chem Senses. 2001; 26:1175–1186. [PubMed: 11705803]

Kanzaki R, Arbas EA, Strausfeld NJ, Hildebrand JG. Physiology and morphology of projection neurons in the antennal lobe of the male moth *Manduca sexta*. J Comp Physiol A. 1989; 165:427–453. [PubMed: 2769606]

Kanzaki R, Shibuya T. Olfactory neural pathway and sexual pheromone responses in the deutocerebrum of the male silkworm moth, *Bombyx mori* (Lepidoptera: Bombycidae). Appl Ent Zool. 1983; 18:131–133.

Kanzaki R, Soo K, Seki Y, Wada S. Projections to higher olfactory centers from subdivisions of the antennal lobe macroglomerular complex of the male silkmoth. Chem Senses. 2003; 28:113–130. [PubMed: 12588734]

Kashiwadani H, Sasaki YF, Uchida N, Mori K. Synchronized oscillatory discharges of mitral/tufted cells with different molecular receptive ranges in the rabbit olfactory bulb. J Neurophysiol. 1999; 82:1786–1792. [PubMed: 10515968]

Kazama H, Wilson RI. Origins of correlated activity in an olfactory circuit. Nat Neurosci. 2009; 12:1136–1144. [PubMed: 19684589]

Khan AG, Thattai M, Bhalla US. Odor representations in the rat olfactory bulb change smoothly with morphing stimuli. Neuron. 2008; 57:571–585. [PubMed: 18304486]

Kohn A, Smith MA. Stimulus dependence of neuronal correlation in primary visual cortex of the macaque. J Neurosci. 2005; 25:3661–3673. [PubMed: 15814797]

Koulakov A, Gelperin A, Rinberg D. Olfactory coding with all-or-nothing glomeruli. J Neurophysiol. 2007; 98:3134–3142. [PubMed: 17855585]

Kruskal PB, Stanis JJ, McNaughton BL, Thomas PJ. A binless correlation measure reduces the variability of memory reactivation estimates. Stat Med. 2007; 26:3997–4008. [PubMed: 17593566]

Kuebler LS, Olsson SB, Weniger R, Hansson BS. Neuronal processing of complex mixtures establishes a unique odor representation in the moth antennal lobe. Front Neural Circuits. 2011; 5:7. [PubMed: 21772814]

Lei H, Christensen TA, Hildebrand JG. Local inhibition modulates odor-evoked synchronization of glomerulus-specific output neurons. Nat Neurosci. 2002; 5:557–565. [PubMed: 12006983]

Lei H, Christensen TA, Hildebrand JG. Spatial and temporal organization of ensemble representations for different odor classes in the moth antennal lobe. J Neurosci. 2004; 24:11108–11119. [PubMed: 15590927]

Lei H, Riffell JA, Gage SL, Hildebrand JG. Contrast enhancement of stimulus intermittency in a primary olfactory network and its behavioral significance. J Biol. 2009; 8:21. [PubMed: 19232128]

Lei H, Reisenman CE, Wilson CH, Gabbur P, Hildebrand JG. Spiking patterns and their functional implications in the antennal lobe of the tobacco hornworm *Manduca sexta*. PLOS ONE. 2011; 6:e23382. [PubMed: 21897842]

Lei H, Vickers N. Central processing of natural odor mixtures in insects. J Chem Ecol. 2008; 34:915–927. [PubMed: 18581181]

Leon M, Johnson B. Functional units in the olfactory system. Proc Natl Acad Sci USA. 2006; 103:14985–14986. [PubMed: 17015819]

Linn C, Campbell M, Roelofs W. The effects of different blend ratios and temperature on the active space of the oriental fruit moth sex-pheromone. Physiol Entomol. 1991; 16:211–222.

Linn CE, Campbell MG, Roelofs WL. Temperature modulation of behavioral thresholds controlling male moth sex-pheromone response specificity. Physiol Entomol. 1988; 13:59–67.

Linn CE, Roelofs WL. Effect of varying proportions of the alcohol component on sex pheromone blend discrimination in male oriental fruit moths. Physiol Entomol. 1983; 8:291–306.

Linn CE, Roelofs WL. Response specificity of male pink-bollworm moths to different blends and dosages of sex-pheromone. J Chem Ecol. 1985; 11:1583–1590.

Löfstedt C, Herrebout WM, Menken SBJ. Sex pheromones and their potential role in the evolution of reproductive isolation in small ermine moths (Yponomeutidae). Chemoecol. 1991; 2:20–28.

Löfstedt C, Pers JN. Sex pheromones and reproductive isolation in four European small ermine moths. J Chem Ecol. 1985; 11:649–666.

Lyttle D, Fellous JM. A new similarity measure for spike trains: Sensitivity to bursts and periods of inhibition. J Neurosci Meth. 2011; 199:296–309.

Machens CK, Stemmler MB, Prinz P, Krahe R, Ronacher B, Herz AVM. Representation of acoustic communication signals by insect auditory receptor neurons. J Neurosci. 2001; 21:3215–3227. [PubMed: 11312306]

Magee JC. Dendritic integration of excitatory synaptic input. Nat Rev Neurosci. 2000; 1:181–190. [PubMed: 11257906]

Martin JP, Hildebrand JG. Innate recognition of pheromone and food odors in moths: a common mechanism in the antennal lobe? Front Behav Neurosci. 2010; 4

Martin JP, Beyerlein A, Dacks AM, Reisenman CE, Riffel JA, Lei H, Hildebrand JG. The neurobiology of insect olfaction: Sensory processing in a comparative context. Prog Neurobiol. 2011; 95:427–47. [PubMed: 21963552]

Mastronarde DN. Interactions between Ganglion-Cells in Cat Retina. J Neurophysiol. 1983; 49:350–365. [PubMed: 6300342]

Matsumoto SG, Hildebrand JG. Olfactory mechanisms in the moth *Manduca sexta*: response characteristics and morphology of central neurons in the antennal lobes. Proc R Soc B. 1981; 213:249–277.

Meister M. Multineuronal codes in retinal signaling. Proc Natl Acad Sci USA. 1996; 93:609–614. [PubMed: 8570603]

Ming QL, Yan YH, Wang CZ. Mechanisms of premating isolation between *Helicoverpa armigera* (Hubner) and *Helicoverpa assulta* (Guenee) (Lepidoptera: Noctuidae). J Insect Physiol. 2007; 53:170–178. [PubMed: 17240394]

Minks AK, Cardé RT. Disruption of pheromone communication in moths - is the natural blend really most efficacious? Entomol Exp Appl. 1988; 49:25–36.

Minks AK, Roelofs WL, Ritter FJ, Persoons CJ. Reproductive isolation of 2 tortricid moth species by different ratios of a 2 component sex attractant. Science. 1973; 180:1073–1074. [PubMed: 17806586]

Najar-Rodriguez AJ, Galizia CG, Stierle J, Dorn S. Behavioral and neurophysiological responses of an insect to changing ratios of constituents in host plant-derived volatile mixtures. J Exp Biol. 2010; 213(19):3388–3397. [PubMed: 20833933]

Nowak LG, Munk MHJ, Nelson JI, James AC, Bullier J. Structural basis of cortical synchronization 1. Three types of interhemispheric coupling. J Neurophysiol. 1995; 74:2379–2400. [PubMed: 8747200]

Olsen SR, Bhandawat V, Wilson RI. Divisive normalization in olfactory population codes. Neuron. 2010; 66:287–299. [PubMed: 20435004]

Paiva ARC, Park I, Principe JC. A comparison of binless spike train measures. Neural Comput Appl. 2010; 19:405–419.

Panzeri S, Brunel N, Logothetis NK, Kayser C. Sensory neural codes using multiplexed temporal scales. Trends Neurosci. 2010; 33:111–120. [PubMed: 20045201]

Perez-Orive J, Mazor O, Turner GC, Cassenaer S, Wilson RI, Laurent G. Oscillations and sparsening of odor representations in the mushroom body. Science. 2002; 297:359–365. [PubMed: 12130775]

Perez-Orive J, Bazhenov M, Laurent G. Intrinsic and circuit properties favor coincidence detection for decoding oscillatory input. J Neurosci. 2004; 24:6037–6047. [PubMed: 15229251]

Perkel DH, Gerstein GL, Moore GP. Neuronal spike trains and stochastic point processes I. The single spike train. Biophys J. 1967a; 7:391–418. [PubMed: 4292791]

Perkel DH, Gerstein GL, Moore GP. Neuronal spike trains and stochastic point processes II. Simultaneous spike trains. Biophys J. 1967b; 7:419–440. [PubMed: 4292792]

Pinault D. A novel single-cell staining procedure performed in vivo under electrophysiological control: Morpho-functional features of juxtacellularly-labeled thalamic cells and other central neurons with biocytin or Neurobiotin. J Neurosci Meth. 1996; 65:113–136.

Puopolo M, Belluzzi O. NMDA-dependent, network-driven oscillatory activity induced by bicuculline or removal of Mg^{2+} in rat olfactory bulb neurons. Eur J Neurosci. 2001; 13:92–102. [PubMed: 11135007]

Quero C, Baker TC. Antagonistic effect of (*Z*)-11-hexadecen-1-ol on the pheromone-mediated flight of *Helicoverpa zea* (Boddie) (Lepidoptera: Noctuidae). J Insect Behav. 1999; 12:701–710.

Riehle A, Grun S, Diesmann M, Aertsen A. Spike synchronization and rate modulation differentially involved in motor cortical function. Science. 1997; 278:1950–1953. [PubMed: 9395398]

Rieke F, Bodnar DA, Bialek W. Naturalistic stimuli increase the rate and efficiency of information transmission by primary auditory afferents. Proc R Soc Lond B. 1995; 262(1365):259–265.

Riffell JA, Lei H, Christensen TA, Hildebrand JG. Characterization and coding of behaviorally significant odor mixtures. Curr Biol. 2009a; 19:335–340. [PubMed: 19230669]

Riffell JA, Lei H, Hildebrand JG. Neural correlates of behavior in the moth *Manduca sexta* in response to complex odors. Proc Natl Acad Sci USA. 2009b; 106:19219–19226. [PubMed: 19907000]

Roelofs WL. Threshold hypothesis for pheromone perception. J Chem Ecol. 1978; 4:685–699.

Roelofs WL, Cardé RT. Responses of Lepidoptera to synthetic sex-pheromone chemicals and their analogs. Annu Rev Entomol. 1977; 22:377–405.

Rolls ET, Tovee MJ, Purcell DG, Stewart AL, Azzopardi P. The responses of neurons in the temporal cortex of primates, and face identification and detection. Exp Brain Res. 1994; 101:473–484. [PubMed: 7851514]

Sanes JR, Hildebrand JG. Structure and development of antennae in a moth, *Manduca sexta*. Dev Biol. 1976; 51:282–299.

Schlyter F, Svensson M, Zhang QH, Knizek M, Krokene P, Ivarsson P, Birgersson G. A model for peak and width of signaling windows: *Ips duplicatus* and *Chilo partellus* pheromone component proportions - does response have a wider window than production? J Chem Ecol. 2001; 27:1481–1511. [PubMed: 11504040]

Schnitzer MJ, Meister M. Multineuronal firing patterns in the signal from eye to brain. Neuron. 2003; 37:499–511. [PubMed: 12575956]

Schoppa NE. AMPA/kainate receptors drive rapid output and precise synchrony in olfactory bulb granule cells. J Neurosci. 2006a; 26:12996–13006. [PubMed: 17167089]

Schoppa NE. Synchronization of olfactory bulb mitral cells by precisely timed inhibitory inputs. Neuron. 2006b; 49:271–283. [PubMed: 16423700]

Schoppa NE, Westbrook GL. Glomerulus-specific synchronization of mitral cells in the olfactory bulb. Neuron. 2001; 31:639–651. [PubMed: 11545722]

Schreiber S, Fellous JM, Whitmer D, Tiesinga P, Sejnowski TJ. A new correlation-based measure of spike timing reliability. Neurocomputing. 2003; 54:925–931. [PubMed: 20740049]

Seki Y, Aonuma H, Kanzaki R. Pheromone processing center in the protocerebrum of *Bombyx mori* revealed by nitric oxide-induced anti-cGMP immunocytochemistry. J Comp Neurol. 2005; 481:340–351. [PubMed: 15593336]

Silbering AF, Galizia CG. Processing of odor mixtures in the *Drosophila* antennal lobe reveals both global inhibition and glomerulus-specific interactions. J Neurosci. 2007; 27:11966–11977. [PubMed: 17978037]

Silbering AF, Okada R, Ito K, Galizia CG. Olfactory information processing in the *Drosophila* antennal lobe: anything goes? J Neurosci. 2008; 28:13075–13087. [PubMed: 19052198]

Silva IM, Eiras AE, Kline DL, Bernier UR. Laboratory evaluation of mosquito traps baited with a synthetic human odor blend to capture *Aedes aegypti*. J Am Mosquito Control Assoc. 2005; 21:229–233.

Singer W. Neuronal synchrony: a versatile code for the definition of relations? Neuron. 1999; 24:49–65. [PubMed: 10677026]

Softky WR, Koch C. The highly irregular firing of cortical-cells is inconsistent with temporal integration of random EPSPs. J Neurosci. 1993; 13:334–350. [PubMed: 8423479]

Swadlow HA, Beloozerova IN, Sirota MG. Sharp, local synchrony among putative feed-forward inhibitory interneurons of rabbit somatosensory cortex. J Neurophysiol. 1998; 79:567–582. [PubMed: 9463422]

Szyszka P, Ditzen M, Galkin A, Galizia CG, Menzel R. Sparsening and temporal sharpening of olfactory representations in the honeybee mushroom bodies. J Neurophysiol. 2005; 94:3303–3313. [PubMed: 16014792]

Tabor R, Yaksi E, Weislogel JM, Friedrich RW. Processing of odor mixtures in the zebrafish olfactory bulb. J Neurosci. 2004; 24:6611–6620. [PubMed: 15269273]

Takahashi S, Sakurai Y. Sub-millisecond firing synchrony of closely neighboring pyramidal neurons in hippocampal CA1 of rats during delayed non-matching to sample task. Front Neural Circuits. 2009; 3:9. [PubMed: 19753324]

Takken W, Dekker T, Wijnholds YG. Odor-mediated flight behavior of *Anopheles gambiae* Giles *Sensu Stricto* and *An. stephensi* Liston in response to CO_2, acetone, and 1-octen-3-ol (Diptera: Culicidae). J Insect Behav. 1997; 10:395–407.

Tasin M, Backman AC, Bengtsson M, Ioriatti C, Witzgall P. Essential host plant cues in the grapevine moth. Naturwissenschaften. 2006; 93:141–144. [PubMed: 16450082]

Tolbert LP, Matsumoto SG, Hildebrand JG. Development of synapses in the antennal lobes of the moth *Manduca sexta* during metamorphosis. J Neurosci. 1983; 3:1158–1175. [PubMed: 6854367]

Trona F, Anfora G, Bengtsson M, Witzgall P, Ignell R. Coding and interaction of sex pheromone and plant volatile signals in the antennal lobe of the codling moth *Cydia pomonella*. J Exp Biol. 2010; 213:4291–4303. [PubMed: 21113011]

Tumlinson JH, Brennan MM, Doolittle RE, Mitchell ER, Brabham A, Mazomenos BE, Baumhover AH, Jackson DM. Identification of a pheromone blend attractive to *Manduca sexta* (L.) males in a wind tunnel. Arch Insect Biochem Physiol. 1989; 10:255–271.

Tumlinson JH, Mitchell ER, Doolittle RE, Jackson DM. Field tests of synthetic *Manduca sexta* sex pheromone. J Chem Ecol. 1994; 20:579–591. [PubMed: 24242113]

Vickers NJ, Christensen TA, Mustaparta H, Baker TC. Chemical communication in heliothine moths 3. Flight behavior of male *Helicoverpa zea* and *Heliothis virescens* in response to varying ratios of intraspecific and interspecific sex-pheromone components. J Comp Physiol A. 1991; 169:275–280.

Vickers NJ, Christensen TA, Hildebrand JG. Combinatorial odor discrimination in the brain: attractive and antagonist odor blends are represented in distinct combinations of uniquely identifiable glomeruli. J Comp Neurol. 1998; 400:35–56. [PubMed: 9762865]

Vinje WE, Gallant JL. Sparse coding and decorrelation in primary visual cortex during natural vision. Science. 2000; 287:1273–1276. [PubMed: 10678835]

Visser JH, Avé DA. General green leaf volatiles in the olfactory orientation of the Colorado beetle, *Leptinotarsa decemlineata*. Entomol Exp Appl. 1978; 24:738–749.

Waldrop B, Christensen TA, Hildebrand JG. GABA-mediated synaptic inhibition of projection neurons in the antennal lobes of the sphinx moth, *Manduca sexta*. J Comp Physiol A. 1987; 161:23–32. [PubMed: 3039128]

Willis MA, Baker TC. Effects of varying sex pheromone component ratios on the zigzagging flight movements of the oriental fruit moth, *Grapholita molesta*. J Insect Behav. 1988; 1:357–371.

Wilson DA, Sullivan RM. Cortical processing of odor objects. Neuron. 2011; 72:506–519. [PubMed: 22099455]

Wu WQ, Anton S, Löfstedt C, Hansson BS. Discrimination among pheromone component blends by interneurons in male antennal lobes of two populations of the turnip moth, *Agrotis segetum*. Proc Natl Acad Sci USA. 1996; 93:8022–8027. [PubMed: 8755596]

Wyatt TD. Pheromones and signature mixtures: defining species-wide signals and variable cues for identity in both invertebrates and vertebrates. J Comp Physiol A. 2010; 196:685–700.

Xu FQ, Greer CA, Shepherd GM. Odor maps in the olfactory bulb. J Comp Neurol. 2000; 422:489–495. [PubMed: 10861521]

Yang CY, Han KS, Boo KS. Sex pheromones and reproductive isolation of three species in genus *Adoxophyes*. J Chem Ecol. 2009; 35:342–348. [PubMed: 19221842]

Yu YG, Romero R, Lee TS. Preference of sensory neural coding for 1/f signals. Phys Rev Lett. 2005; 94:103–108.

Zavada A, Buckley CL, Martinez D, Rospars JP, Nowotny T. Competition-based model of pheromone component ratio detection in the moth. PLOS One. 2011; 6:e16308. [PubMed: 21373177]

Abbreviations

AL	antennal lobe
BAL	bombykal (E,Z-10,12-hexadecadienal)
EAG	electroantennogram
EEZ	E,E,Z-10,12-14-hexadecatrienal
MGC	macroglomerular complex
mPN	multi-glomerular projection neuron
ORC	olfactory receptor cell
PN	projection neuron
uPN	uniglomerular projection neuron
VOC	volatile organic compound

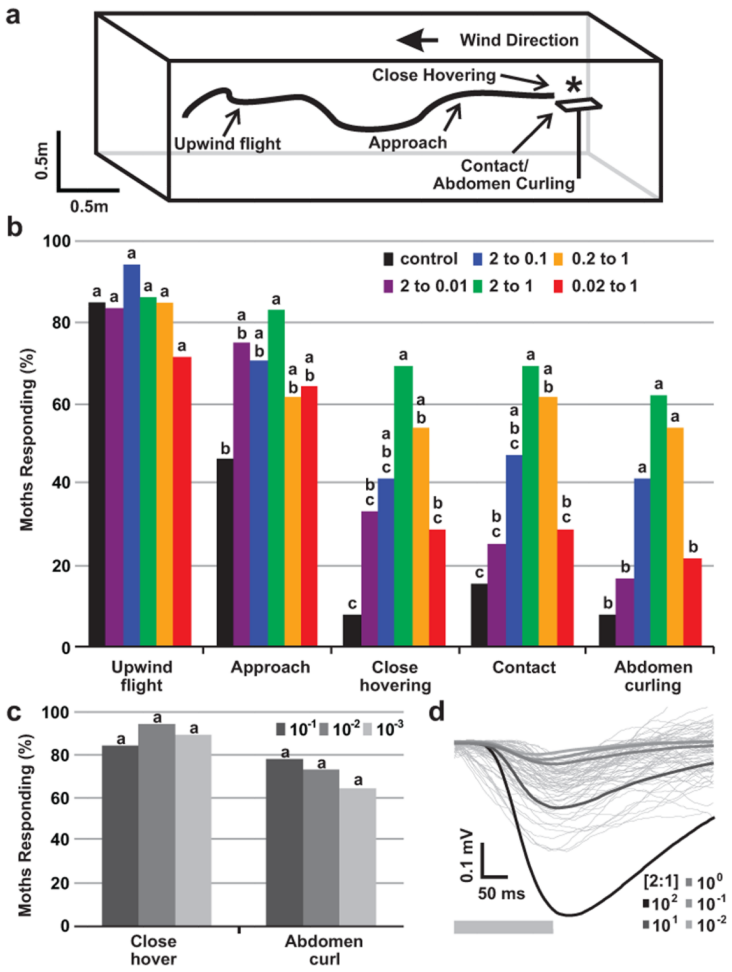

Fig. 1.

Behavioral responses of male moths to mixtures with various ratios of pheromone components. **a** Schematic drawing of the wind tunnel used for behavioral experiments, with scored behaviors indicated along a simulated flight path: Upwind Flight, Approach, Close Hovering, Contact, and Abdomen Curling. The pheromone source (lure) is indicated by an *asterisk*. **b** Frequency of scored responses to control (cyclohexane) and each of 5 mixtures with varied ratios between the two components. Bars with the same letter are not significantly different (at P<0.05, Fisher exact test). Differences within treatments: Upwind flight, X^2=3.133, P=0.679; Approach, X^2=6.483, P=0.262; Close hovering, X^2=16.773, P=0.005; Contact, X^2=16.181, P=0.006; Abdomen curling, X^2=22.888, P<0.001. **c** Behavioral responses to dilutions of the 2:1 mixture (BAL:EEZ). Behavioral frequencies were not different from each other (at P<0.05, Fisher exact test), nor was the difference among treatments significant (at P<0.05, Chi square test). **d** EAG waveforms recorded in the wind tunnel evoked by the 2:1 (BAL:EEZ) mixture at a distance of 30 cm (*thin, light grey traces*), overlaid by the average EAGs recorded in the physiological rig evoked by 0.03, 0.3, 3, 30, and 300 ng of the 2:1 mixture (BAL:EEZ) (*greyscale traces; grey bar* indicates stimulus period in physiological experiments).

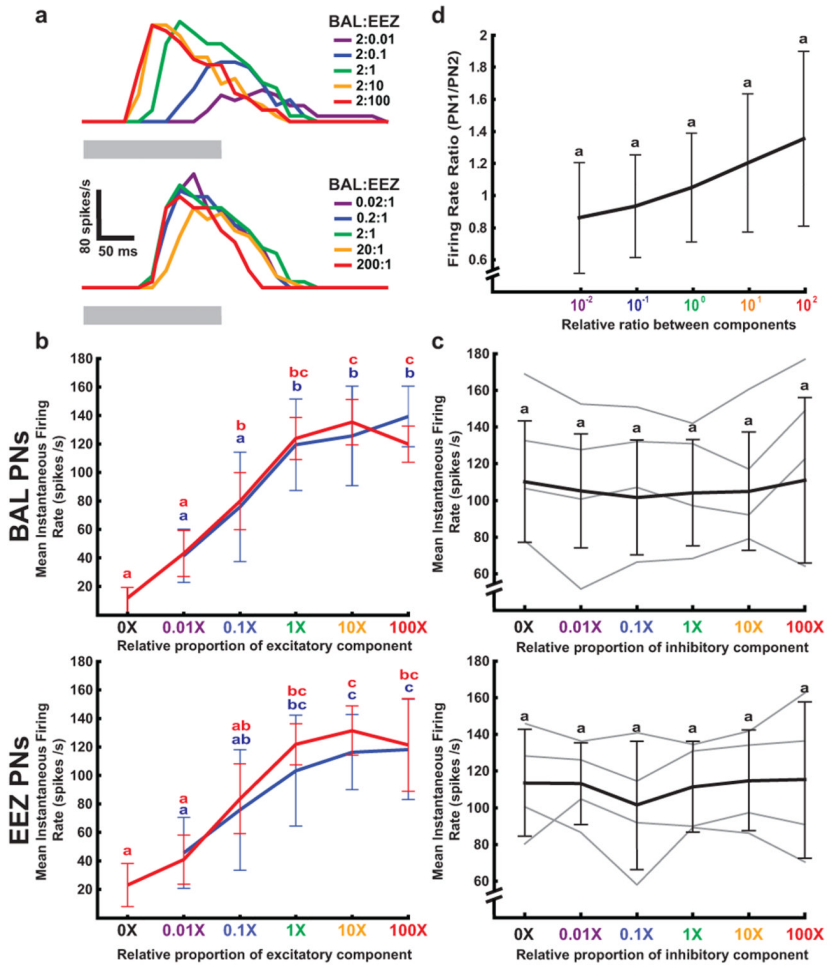

Fig. 2.

Firing rate responses of individual PNs form a poor representation of the ratio between components in a pheromone mixture. **a** Peri-stimulus time histograms of a representative PN selective for the EEZ component of the pheromone. *Top*: Responses to mixtures with increasing concentration of the EEZ (excitatory) component. *Bottom*: Responses to mixtures with increasing concentration of the BAL (inhibitory) component (*grey bar*, 200 ms stimulus). **b** Population averages of the mean instantaneous firing rate of individual PNs (BAL-PNs, *top*, n = 20; EEZ-PNs, *bottom*, n = 4) in response to mixtures with increasing proportion of the excitatory component (BAL, *top*; EEZ, *bottom*) alone (*blue line*) and in a mixture with a constant concentration of the inhibitory component (EEZ, *top*; BAL, *bottom*) (*red line*). Letters indicate means that were not significantly different (Tukey test, $P<0.05$, n = 21). The variance was significantly reduced in response to the 1× concentration of the excitatory component mixed with the inhibitory component relative to the excitatory component alone for both types of PNs (Levene's test, $P<0.05$). **c** Population averages of the mean instantaneous firing rate of individual PNs (BAL-PNs, *top*, n = 20; EEZ-PNs, *bottom*, n = 4) in response to mixtures with increasing proportion of the inhibitory component (EEZ, *top*; BAL, *bottom*) (*thick, black line*) and the responses of a selection of individual PNs (*thin, grey lines*). The effect of the proportion of the inhibitory component was not significant (Friedman repeated measures ANOVA, $P>0.05$). **d** Firing-rate ratios calculated between randomly paired PNs from the entire population responding to different

concentrations of their excitatory component. The effect of the relative ratio between components was not significant (Friedman repeated measures ANOVA, $P>0.05$).

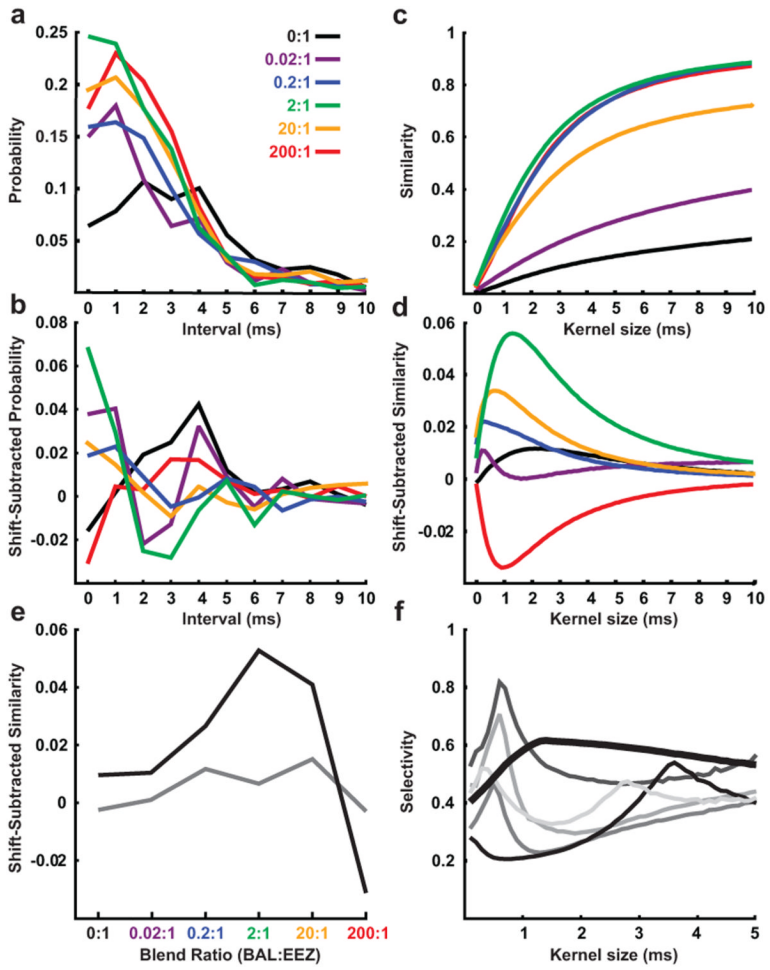

Fig. 3.

Synchrony between pairs of PNs is modulated by the ratio between pheromone components in a mixture. **a-b** Raw and shift-predictor subtracted cross-interval histograms for a representative PN pair selective for the EEZ component in response to mixtures with increasing concentration of the inhibitory (BAL) component. **c-d** Raw and shift-predictor-subtracted similarity index from the PN pair in **a-b. e** Synchrony responses of the PN pair in **a-d** to a series of pheromone component ratios at the maximum (*black line*) and minimum (*grey line*) selective kernel widths. **f** Selectivity index for the similarity-based measure of synchrony between the PN pair in **a-d** (*thick line*) and a selection of 5 other PN pairs (*thin, grey lines*).

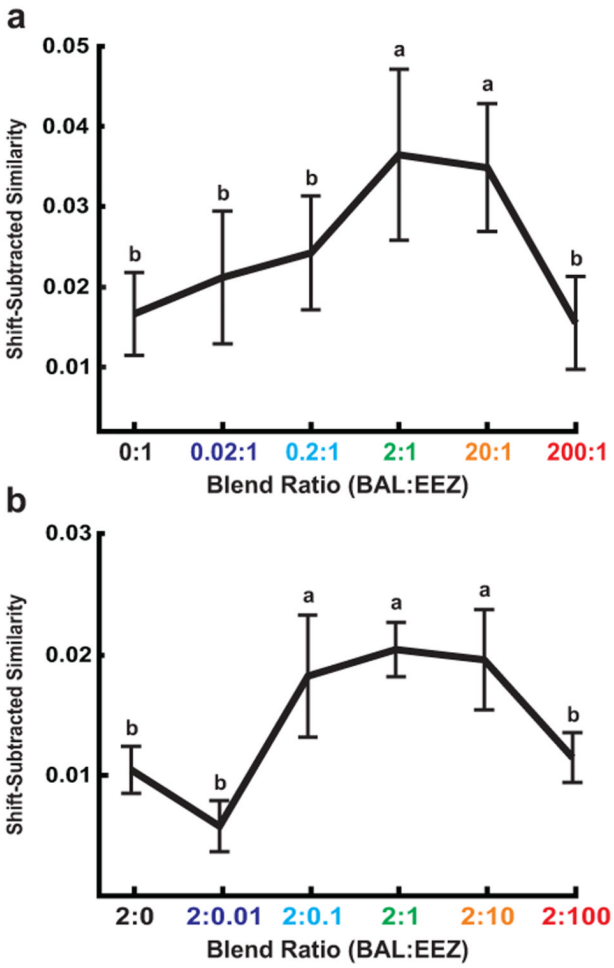

Fig. 4.

Spiking synchrony across the recorded population of PNs is maximal in the behaviorally effective range of pheromone-component ratios. The mean shift-predictor-subtracted similarity (±SEM) across all pairs of PNs exhibiting ratio-selectivity in response to mixtures in which either BAL (**a**) or EEZ (**b**) was altered (n = 12 pairs).

Table 1

Stimuli used in behavioral experiments

Mixture (BAL:EEZ)	Concentration of component		Moths tested
	BAL	EEZ	
cyclohexane control	0 ng/μl	0 ng/μl	n = 13
2:0.01	200 ng/μl	1 ng/μl	n = 12
2:0.1	200 ng/μl	10 ng/μl	n = 17
2:1	200 ng/μl	100 ng/μl	n = 29
0.2:1	20 ng/μl	100 ng/μl	n = 13
0.02:1	2 ng/μl	100 ng/μl	n = 14
Serial Dilutions			
10^{-1} (2:1)	20 ng/μl	10 ng/μl	n = 12
10^{-2} (2:1)	2 ng/μl	1 ng/μl	n = 12
10^{-3} (2:1)	0.2 ng/μl	0.1 ng/μl	n = 12

Table 2

Stimuli Used In Physiological Experiments

		Concentration of component			Concentration of component	
	BAL Mixtures	**BAL**	**EEZ**	**EEZ Mixtures**	**BAL**	**EEZ**
	cyclohexane	0 ng/μl	0 ng/μl	cyclohexane	0 ng/μl	0 ng/μl
Component alone	0.02:0	0.2 ng/μl	0 ng/μl	0:0.01	0 ng/μl	0.1 ng/μl
	0.2:0	2 ng/μl	0 ng/μl	0:0.1	0 ng/μl	1 ng/μl
	2:0	20 ng/μl	0 ng/μl	0:1	0 ng/μl	10 ng/μl
	20:0	200 ng/μl	0 ng/μl	0:10	0 ng/μl	100 ng/μl
	200:0	2000 ng/μl	0 ng/μl	0:100	0 ng/μl	1000 ng/μl
Mixture	0.02:1	0.2 ng/μl	10 ng/μl	2:0.01	20 ng/μl	0.1 ng/μl
	0.2:1	2 ng/μl	10 ng/μl	2:0.1	20 ng/μl	1 ng/μl
	2:1	20 ng/μl	10 ng/μl	2:1	20 ng/μl	10 ng/μl
	20:1	200 ng/μl	10 ng/μl	2:10	20 ng/μl	100 ng/μl
	200:1	2000 ng/μl	10 ng/μl	2:100	20 ng/μl	1000 ng/μl